

TOPICAL REVIEW

Memristive Biosensors for Cancer Biomarkers Detection: A Review

RAMI HOMSI^{1,2}, NOSAYBA AL-AZZAM³, BAKER MOHAMMAD^{1,4}, (Senior Member, IEEE), AND ANAS ALAZZAM^{1,2}

¹System on Chip Laboratory (SoCL), Khalifa University, Abu Dhabi, United Arab Emirates

²Department of Mechanical Engineering, Khalifa University, Abu Dhabi, United Arab Emirates

³Department of Physiology and Biochemistry, Jordan University of Science & Technology, Irbid 22110, Jordan

⁴Department of Electrical Engineering and Computer Science, Khalifa University, Abu Dhabi, United Arab Emirates

Corresponding author: Anas Alazzam (anas.alazzam@ku.ac.ae)

This work was supported by the Khalifa University of Science and Technology under Award RC2-2018-020.

ABSTRACT Detecting cancer biomarkers at an early stage at the clinical level has been the interest of numerous researchers over the years due to its impact on recovery. Therefore, attention is towards fabricating reliable, cost-effective, reproducible, and accurate devices for point-of-care screening. This review aims to highlight the emerging field of memristive biosensors and compare it to similar electrochemical devices used for cancer biomarker detection. The limit of detection (LOD) achieved by memristive biosensors was generally in the femtomolar (fM) range in comparison to field effect transistors (FET) and electrochemical immunosensors, which in most instances exhibited a LOD in the picomolar (pM) and nanomolar (nM) range. Most current memristive biosensors are fabricated using silicon nanowires, which calls for exploring different materials and structures that may lower fabrication complexity and increase reproducibility. This article examines the working principle of memristors for biosensing, the biofunctionalization of antibodies, the interaction between antibodies and antigens and its influence on memristors, as well as fabrication processes and applications of memristors for biosensing. This paper will report on memristor-based biomedical sensors focusing on cancer screening. In addition, the outlook of reduced graphene oxide (rGO) as an active material for sensing will be discussed. Memristors are anticipated to enhance the future of sensing due to their great sensitivity and simplicity of fabrication.

INDEX TERMS Cancer, biomarker, biosensing, memristor, antigens, rGO.

I. INTRODUCTION

The detection, characterization, and separation of different particles and cells, including cancer cells, have gained tremendous attraction from researchers in the past few decades in pursuit of fabricating more effective and efficient devices. Different separation techniques, like dielectrophoresis (DEP) [1], acoustophoresis (ACP) [2], magnetophoresis (MAP) [3], optophoresis (OPP) [4], hydrophoresis (HYP) [5], and deterministic lateral displacement (DLD) [6], were used to fabricate devices for the separation of different microparticles. The mentioned separation techniques have various applications and utilize distinct criteria or characteristics of the target cells for their separation/capture.

The associate editor coordinating the review of this manuscript and approving it for publication was Santosh Kumar¹.

Another field of interest is detecting and characterizing different cancer biomarkers using biosensors [7], [8], [9]. These biosensors usually have two main components: a bioreceptor and a transducer. The bioreceptor is a biomolecule attached to the device that recognizes the target molecule, while the transducer transfers a signal containing this identification process [10]. The signal measured determines the type of biosensor, which could be mechanical [11], optical [12], electrochemical [13], or electrical [14]. Many biosensing studies have been conducted on one of the electrical biosensors, namely the field effect transistor (FET) since it is a good candidate for point-of-care (POC) devices [15], [16], [17]. FETs are usually composed of three main terminals: the source, drain, and gate. These devices are used as biosensors, utilizing the idea that a measurable change in device electrical characteristics will occur due to a reaction between the

bioreceptor and the biological analyte being sensed. Some of the biological analytes will attach to the bioreceptors, changing the charge carrier concentration of the conducting material in use. Composite immunosensor electrodes are another electrochemical device used as biosensors that detect target analytes in a sample by combining recognition elements, such as antibodies, and a transduction mechanism, such as an electrode. To enhance the overall functionality of the biosensor, the transduction mechanism, usually an electrode, may be altered with additional components, such as enzymes, and composed of different materials, such as gold or carbon.

Another emerging technology or device used in molecule sensing, and particularly in cancer biomarker sensing, is the memristor. As the name suggests, the memristor is essentially a resistor with a memory. This device was used as a biosensor in multiple studies, exhibiting high sensing accuracy [18], [19], [20]. Recently, Carrara [21] published a review in the field of memristors, highlighting the new interest and increase in research on memristors and the different types of memristor sensors, mainly physical and chemical memristor sensors.

This article provides a comprehensive overview of memristor biosensing applications. Memristive biosensors used for the detection of cancer biomarkers like Prostate specific antigen (PSA), Carcinoembryonic antigen (CEA), and Vascular Endothelial Growth Factor (VEGF) will be reviewed in depth. To the best of the authors' knowledge, a review of the current state of memristive biosensors used to detect cancer biomarkers is unavailable in the literature. Consequently, this review aims to provide a detailed overview of the current memristive biosensors and compare them to traditional electrochemical biosensors. Initially, the general history and working principles of memristors will be presented in Section II. Section III will focus on the specific detection principle of memristive biosensors, bio-functionalization of antibodies, and antibody-antigen interaction. In addition, state-of-the-art works on biomarker detection using memristive biosensors, fabrication of silicon nanowires, comparison of memristors with other types of biosensors, and the advantages and limitations of memristive biosensors will be discussed in Section IV. Finally, conclusions and future recommendations in this emerging field of memristor biosensors will be highlighted in Section V.

II. THEORY OF MEMRISTORS

A. MEMRISTOR HISTORY

Leon Chua first described the memristor theoretically and given its name in 1971 [22]. Leon Chua pointed out in his paper that the theory of circuits seems to be missing a fourth component. This component had to relate the magnetic flux (φ) with charge (q) since all other possible governing parameters, i.e., voltage, current, charge, and magnetic flux, are already related by established essential components,

namely, the resistor which connects voltage to current, the capacitor which relates voltage to charge, and inductor which relates current to flux. That said, this was not the first time a device with memristor qualities was established; such a device was shown in late 1800, as indicated by Prodromakis [23].

Although the memristor was first theoretically established and named in 1971, it was first fabricated in 2008 by Strukov et al. [24]. Since then, utilizing memristors in different applications has been pursued by many researchers, and numerous works have been published throughout the years, as shown in Figure 1. The category "Total" data in the figure is derived from Scopus using the keyword "memristor/s" in the manuscript's title or keywords. The data for the Sensors and Biosensors categories were acquired using the same methodology, with the addition of having the keywords "sensor/s" and "biosensor/s" in the title, abstract, or keywords of the articles. The figure shows the current state of memristors, which receive great attention with the growing number of papers published yearly. The pie chart in Figure 1 shows the different applications where memristors are utilized with their respective percentages. Those applications include studies on neural networks [25], [26], [27], [28], resistive switching [29], [30], [31], [32], chaotic circuits [33], [34], [35], [36], and sensing, which includes temperature sensing [37], force sensing [38], radiation sensing [39], and gas sensing [40]. The category named "Other" in Figure 1 includes and is not limited to applications like material science [41], probabilistic computing [42], and numerical computing [43].

B. WORKING PRINCIPLE

In simple terms, a memristor can be defined as a resistor that changes resistance as you apply voltages. As established by [22], the voltage across a memristor as a function of charge is given by

$$v(t) = M(q(t))i(t) \quad (1)$$

where the memristance $M(q)$ is defined as

$$M(q) = d\varphi(q)/dq \quad (2)$$

Analogously, the current through a memristor as a function of flux is given by

$$i(t) = W(\varphi(t))v(t) \quad (3)$$

where the memductance $W(\varphi)$ is defined as

$$W(\varphi) = dq(\varphi)/d\varphi \quad (4)$$

This property is summed up by applying a sweeping voltage across the device and measuring the current as a function of voltage; this will result in the pinched hysteresis loop as shown in Figure 2.

As the voltage increases, the current increases linearly as a function of the voltage, and it has a shallow slope, indicating that its conductance is low. After that, it reaches a threshold

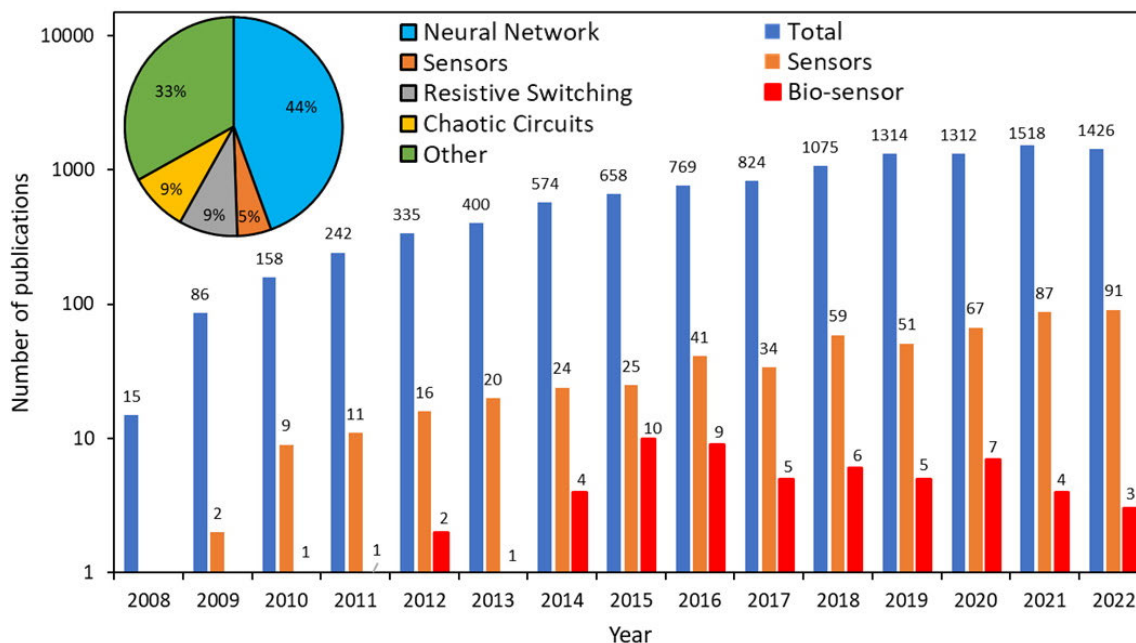


FIGURE 1. Number of publications per year on memristors (log scale) and pie chart showing the different categories of studies conducted using memristors. Data were obtained from Scopus.

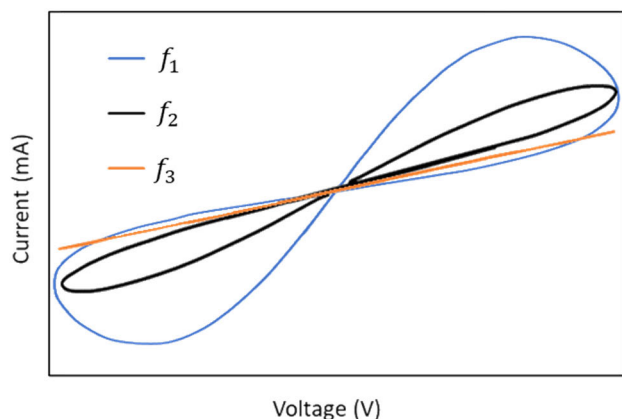


FIGURE 2. Illustration of current versus voltage for a standard memristor at different frequencies, $f_1 < f_2 < f_3$.

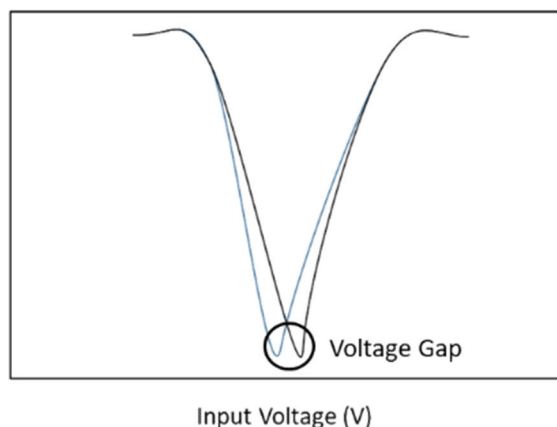


FIGURE 3. Illustration of logarithmic current against voltage for a functionalized memristor biosensor showing the voltage gap.

of adaptation, and the conductance increases, as indicated by the steeper slope. These two slopes indicate two different resistive or conductive states. As the voltage sweeps back down, it is in a higher conductance state, and the polarity reverses, where a reverse adaptation threshold is reached, causing the conductance to decrease. The fact that the pinched hysteresis loop goes through the origin implies that the device is not storing energy and holds the memory of the last voltage applied to it.

III. MEMRISTIVE BIOSENSORS WORKING PRINCIPLES

A. DETECTION PRINCIPLE

The detection of biomarkers using memristors is similar to that of FETs, where a change in conductance

occurs due to bioreceptor and biological analyte binding, as explained in Section I. However, in the case of memristors, the attachment (bio-functionalization) of charged residues like antibodies on the surface of the device causes a gap in the logarithmic current-voltage curve, as indicated in Figure 3.

Like FETs, this gap in the voltage-current curve of memristors is due to a change in the device's conductance. The attachment of proteins (antibodies) can be viewed as a virtual gate that controls the current. While applying a positive gate voltage causes carriers to be depleted and the conductance to decrease for a p-type device, doing so while using a negative gate voltage causes carriers to build up and the conductance to increase. During antigen

uptake, the voltage gap gets smaller because the antigen binding to antibodies (which happens when antigen and antibodies interact) hides the effect that antibodies are already giving.

The change in electrical properties upon antigen-antibody binding on a device could also be caused when the electric field acts as an energy source for the fluid, resulting in AC electroosmosis (ACEO), a type of alternating current (AC) electrokinetic forces. This force could create swirling structures in the fluid, which will enhance the delivery of the analyte to the immunosensor device's reaction surface [44].

B. BIO-FUNCTIONALIZATION OF ANTIBODIES

Memristive devices used in biosensing are usually functionalized with antibodies to detect antigens through a change in the voltage gap in the devices' response due to antibody-antigen interaction. Four main techniques exist in the literature for the attachment of antibodies on the surface of a device, namely direct adsorption [20], [45], [46], affinity approach [47], covalent attachment using Glycidoxypropyltrimethoxysilane (GPTS) [18], [48], [49], covalent attachment using 1-(3-(Dimethylamino)propyl)-3-ethyl carbodiimide hydrochloride (EDC) and N-hydroxysulfosuccinimide (NHS) [16], [50], [51], [52], [53], [54], [55], and non-covalent attachment [17]. The direct adsorption technique usually starts by treating the device with oxygen plasma for 15 minutes to increase hydroxyl groups (OH-). Subsequently, the device is exposed to a solution of target antibody in phosphate-buffered saline (PBS) and incubated for multiple hours. Finally, the device is washed with PBS and gently dried with nitrogen. This process is graphically depicted in Figure 4 (a). The affinity approach is presented in Figure 4 (b), where the process starts by exposing the device to a solution of PBS containing biotin to immobilize biotin on the surface. Then, streptavidin is attached to the surface on top of the existing biotin. Finally, the biotinylated aptamer is immobilized on the device's surface.

Covalent attachment is the predominant type of functionalization used for cancer biomarker sensing, as will be highlighted later in this review. Covalent attachment can be achieved by using either GPTS or EDC and NHS. The first technique using GPTS starts by exposing the device to ethanol, acetic acid, and GPTS. Subsequently, the device is washed multiple times with ethanol and acetic acid, dried with nitrogen, and heated in an oven. Finally, ethanolamine is used to block any remaining GPTS groups active on the surface.

On the other hand, covalent attachment using EDC and NHS starts with treating the device with oxygen plasma to increase OH- groups for better binding. After that, the device is immersed in an ethanol solution and later exposed to the target antibody in PBS, EDC, and NHS solution for multiple hours. Finally, the device is washed with PBS and gently dried with nitrogen flow. At this point, the device

is ready for incubation successively in solutions of antigen in PBS for antigen uptake. A graphical representation of the covalent attachment using EDC and NHS is presented in Figure 4(c).

Non-covalent attachment can be done through π -stacking, like the interaction of graphene with the 1-pyrenebutanoic acid succinimidyl ester (PYR-NHS), as shown in Figure 4 (d) [17]. Initially, to establish a linker, a device is exposed to a dimethylformamide (DMF) solution with PYR-NHS and washed with DMF afterwards. Then, the device is incubated in a solution of PBS with the target antibody for multiple hours. Finally, the device is washed with PBS and exposed to ethanolamine to block any remaining activated groups on the surface of the device.

A study related to the attachment of antibodies was presented by Tzouvadaki et al. [56], where they studied the effect of different bio-functionalization techniques on the performance of silicon nanowire memristors taking anti-Prostate Specific Antigen (PSA) antibodies as a case study. Their work showed that the direct adsorption functionalization technique performed almost two times better than the affinity approach and covalent linkage at high humidity ratios.

C. INTERACTION OF ANTIGENS AND ANTIBODIES

Antibodies are Y-shaped proteins that are required for an immune response. Antibodies recognize antigens with high specificity, making them ideal therapeutic targets [57]. Antibody-antigen complexes exhibit a high degree of shape and chemical complementarity at their interacting surfaces. Hydrophobic regions on the antigen surface interact with hydrophobic regions on the antibody combining site, polar atoms engage with polar atoms across the interface, and proton donors and acceptors establish hydrogen bonds. Protruding side chains on one surface nestle into depressions on the other, and numerous van der Waals interactions are interspersed with hydrogen bonds and the occasional salt bridge [58].

Antibodies are classified into two types: polyclonal antibodies and monoclonal antibodies [59]. Polyclonal antibodies, also known as antiserum antibodies, are produced from the products of numerous B-lymphocytes from animals (in vivo), are less sensitive to epitope variations, and are specific with some cross-reactivity. On the other hand, a monoclonal antibody is produced using both in vivo and in vitro systems and is characterized by its high sensitivity, specificity, and lack of cross-reactivity. Furthermore, when compared to polyclonal reagents, monoclonal reagents are more complicated and expensive to produce in the long term [59], [60].

Circulating immune complexes composed of tumour antigens and immunoglobulin M (IgM) are a novel class of biomarkers with diagnostic significance for the early detection of cancer [61]. Antigenic components of circulating immune complexes have been found to arise from diseased tissues in most malignancies. As the illness advances, these

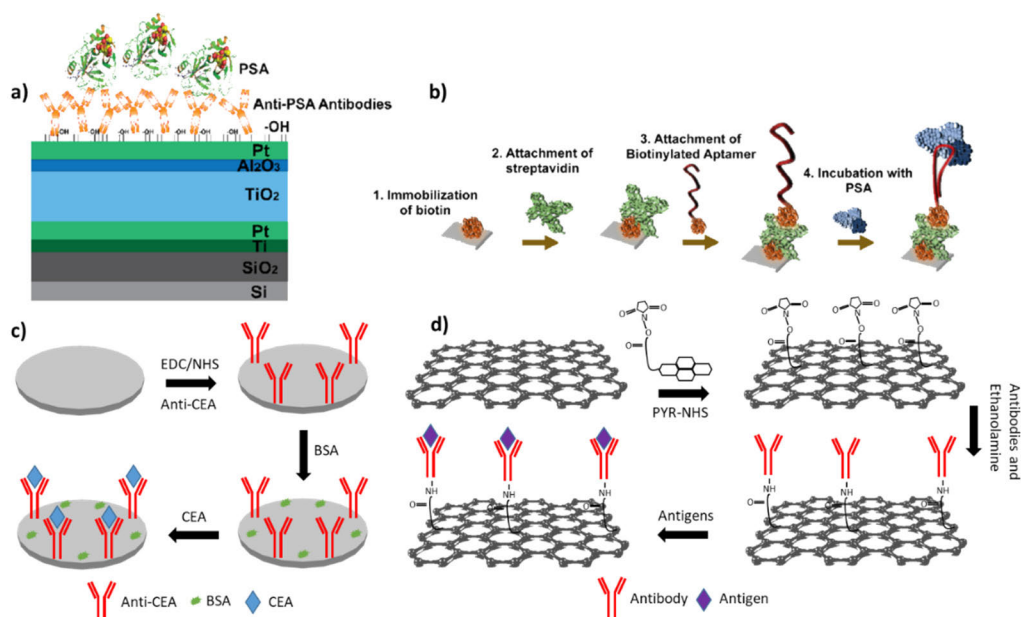


FIGURE 4. a) Bio-functionalization of PSA antibody using direct adsorption technique, figure taken from [20]. (b) Affinity approach for the surface attachment of PSA antibody. Reprinted with permission from [47]. Copyright (2016) American Chemical Society. (c) Covalent attachment of carcinoembryonic antigen (CEA) antibody using EDC and NHS. Illustration of methodology used in [54]. (d) Non-covalent attachment of CEA antibody through π -stacking by the interaction of graphene with PYR-NHS. Illustration of methodology used in [17].

tissues shed more antigens, which is believed to increase the concentration of circulating immune complexes [62]. In the cases of prostate cancer [63], colorectal cancer [64] and liver cancer [65], [66], [67], tumour biomarkers are responsible for the development of circulating tumour-related antigens-IgM complexes. Examining these circulating immune complexes performed better than analyzing the comparable free biomarker [68]. Cirrhosis and hepatocellular cancer (HCC) may develop in patients infected with the hepatitis B (HBV) or C (HCV) viruses. As a result, patients must be regularly evaluated using serum alpha-fetoprotein (AFP) determinations and liver ultrasounds every six months to detect HCC nodules. The appropriate AFP cut-off level for the diagnosis of HCC is still debatable. Some studies used 20 ng/mL, and others favoured the 200 ng/mL or 400 ng/mL concentration [69]. Another biomarker for monitoring cirrhosis and HCC that has been proven to work is the immune complex made up of Squamous Cell Carcinoma Antigen and IgM (SCCA-IgM) [67]. 120 AU/mL was the optimal SCCA-IgM threshold for discriminating between HCC-free and overall survival rates. Patients whose baseline levels exceeded this threshold demonstrated a significant increase in both the HCC incidence and all-cause death rates. Patients with higher baseline SCCA-IgM values (>120 AU/mL) were more likely HCV-positive and had higher blood AFP levels [70].

In the case of colorectal cancer, the carcinoembryonic antigen-IgM complex (CEA-IgM) is used as a biomarker for the early detection of the disease [64]. However, CEA is also elevated in other types of cancer, such as lung [71]

and breast [72] cancers. A free CEA reading of 5.0 ng/mL and a CEA-IgM complex level of 200 AU/mL are considered elevated. However, a particular cut-off value is not available. Colorectal cancer is associated with higher CEA and CEA-IgM levels [64].

Another biomarker is the Vascular Endothelial Growth Factor (VEGF) which is a decisive angiogenesis factor and is generally linked to the growth and metastasis of tumours [73], [74] and specifically for the diagnosis of breast cancer [75], [76]. Endothelial cells, smooth muscle cells, fibroblasts, and cancer cells are some of the cells that produce VEGF in the human body. Further, circulating serum cancer antigen 125 (CA125) has been identified as a biomarker of ovarian cancer and is used for screening epithelial-type ovarian cancer [77], [78]. The threshold value for CA125 is 35 U/mL, and their higher levels were correlated mainly with ovarian and other cancer types [79], [80].

In prostate cancer screening, the first line and most often utilized serum biomarker is prostate-specific antigen (PSA). Prostate cancer is the second most common male malignancy and the sixth leading cause of cancer death [81]. PSA is an enzyme that the glandular tissue of the prostate typically produces. The PSA test has an overall sensitivity of about 20% and a specificity of about 60% to 70% when using a threshold of more than 4.0 ng/mL [82], [83]. Testing for serum levels of the PSA-IgM immunological complex has been shown to enhance the diagnostic performance of total PSA in prostate cancer. The combination of PSA-IgM and total PSA is the best technique for reducing the number of

TABLE 1. Biomarkers with their sources in the human body, associated types of cancer, and concentration threshold values.

Biomarker	Source	Type of Cancer	Threshold Value	Ref
CEA	Cancer cells	Colorectal, lung, or breast	5 ng/mL	[64]
VEGF	Endothelial cells, smooth muscle cells, fibroblasts, and cancer cells	Breast	-	[75, 76]
PSA	Glandular tissue of prostate	Prostate	4 ng/mL	[82, 83]

negative prostatic mappings and thereby improving prostate cancer diagnosis [84]. Most modern PSA detection assays are run on big analyzers at specialized testing facilities, requiring samples to be transported away for analysis. This causes delays in patient care and increases administrative expenditure. The growing importance of managing patients at the point of care has led to the development of new biosensor detection techniques that are perfect for reducing the size of assays for different targets, including PSA [85]. The associated biomarkers, cancer type, and threshold values are listed in Table 1. It is noted that the VEGF concentration threshold for breast cancer is not well defined and may vary based on the stage and type of breast cancer. Increased angiogenesis (the formation of new blood vessels) and a poor prognosis in breast cancer patients have been linked to elevated levels of VEGF. Nevertheless, more research is required to pinpoint a precise VEGF threshold concentration that would signal the presence or severity of breast cancer.

Thermodynamic parameters reflect the state with the lowest Gibbs free energy (G°) under equilibrium. A significant negative shift in standard G° upon engagement characterizes a strong molecular interaction. The change is expressed as the sum of the experimentally determined changes in enthalpy (H°) and entropy (S°). The standard enthalpy change upon antibody-antigen interaction is primarily associated with the non-covalent bond formation and conformational change. On the other hand, bound water molecule behaviour and the conformational flexibility of the antibody or antigen are frequently associated with the standard entropy change [86]. At room temperature or lower, the antigen-antibody reaction is usually exothermic (releases heat), but H can range from -20 to 10 kcal/mol [87]. Further, a thermodynamic study contributes to the picture by shedding light on the molecular forces involved in the antigen-antibody interaction. Understanding the specific molecular interactions that occur in systems involving mutagenized antigen or antibody molecules allows for developing improved diagnostic or therapeutic reagents [88].

IV. BIOMARKER DETECTION

A. MEMRISTOR STUDIES ON DETECTION OF BIOMARKERS

Most studies conducted on memristive biosensors utilized silicon nanowires sensors. Some early memristive biosensing studies were conducted on rabbit antigens as a proof of concept or case study. Carrara et al. [18] were the first to utilize the memristive effect for biosensing. Silicon nanowires fabricated through the top-down technique were functionalized covalently with rabbit polyclonal antibodies to detect rabbit antigens. Using the change in voltage gap when exposing the memristor to different concentrations of rabbit antigens, they achieved a sensitivity and limit of detection (LOD) of 37 ± 1 mV/fM and 3.4 ± 1.8 fM, respectively. Tzouvadaki et al. [89] fabricated a multi-panel chip capable of biosensing through electrical (memristor) and fluorescent characterization techniques. This device is considered a pathway to point-of-care (POC) devices since it can detect single or multiple biomarkers from a sample containing various target and non-target molecules using several characterization techniques. The device was shown to successfully detect rabbit antigens at a LOD of 1.6 fM in a sample containing three other negative control reagents through a voltage gap change.

Many studies utilizing silicon nanowire memristors focused on the biosensing of cancer biomarkers like Vascular Endothelial Growth Factor (VEGF) and Prostate Specific Antigen (PSA). Puppo et al. [48], [49] fabricated memristive silicon nanowires with Nickel Silici, creating a Schottky-barrier at their terminals. The effect of humidity variation on covalently functionalized silicon nanowires with anti-Vascular Endothelial Growth Factor (VEGF) antibodies was investigated. They found that unfunctionalized (bare) devices exhibited a voltage gap of almost zero at all humidity levels tested, while the voltage gap of devices functionalized with antibodies changed significantly with a change in humidity. The covalently functionalized memristors could detect VEGF at concentrations of 0.6 to 2.1 fM. Tzouvadaki et al. [47] were the first to fabricate memristive silicon nanowires functionalized with DNA aptamers to detect PSA. Their device exhibited a LOD of 23 aM, the lowest achieved for detecting PSA using an electrochemical sensor. This LOD surpasses the current sensitivity of the clinical tests available for PSA [90]. Tzouvadaki et al. [91], [92] fabricated memristive silicon nanowire sensors to detect PSA-immunoglobulin M (IgM) through direct adsorption of an anti-PSA antibody. PSA complexed with IgM is another significant biomarker, along with free PSA present in the serum of cancer patients. In the second study [92] electrical characterization through a voltage gap difference and enzyme-linked immunosorbent assay (ELISA) tests were conducted to detect PSA-IgM at concentrations as low as 11.75 AU/mL. Tzouvadaki et al. [19] proposed a memristive biosensing board prototype containing a sensor module, ADC, MUX, microcontroller, data storage, and power supply. The biosensing component comprises 12 identical memristive nanowires, each producing a distinct

signal, while all sensors are excited by the same common source. The device was functionalized with an anti-PSA antibody and achieved a LOD of 3.3 fM, where the critical value of PSA is approximately 133 pM. In a recent study, Tzouvadaki et al. [93] studied the differences in the detection of PSA using memristive nanowires functionalized with three bio-probes, namely anti-PSA single-chain antibody fragment, anti-PSA full-chain antibody, and anti-PSA DNA-aptamers. They found that the voltage gap of the device increases linearly with the size of the reagent on its surface. The memristor achieved the lowest detectable concentration of 4.8 fM based on an anti-PSA single-chain antibody fragment.

Non-cancer biomarkers like Tenofovir and Ebola virus were also detected using memristive biosensors utilizing silicon nanowires. Tzouvadaki et al. [94] utilized memristive silicon nanowires fabricated through both top-down and bottom-up techniques and functionalized with DNA-aptamers to detect the antiviral drug Tenofovir. They focused on detecting Tenofovir in a buffer and full human serum, where a LOD of 3.09 pM and 1.38 nM was achieved, respectively. Ibarlucea et al. [50] fabricated a memristive honeycomb-shaped silicon nanowire functionalized with an Ebola VP40 matrix antibody. The device detected the Ebola VP40 protein (virus) by utilizing the pinched hysteresis in the voltage versus current response at a limit of 6 fM.

All previously discussed studies on memristors have been limited to the use of silicon nanowires. However, Hadis et al. [95], [96] fabricated a composite immunosensor device with a microfluidic channel to detect non-structural protein 1 (NS1 protein) as a biomarker that aids in the early detection of the dengue virus. The device consisted of a glass substrate, indium tin oxide (ITO), titanium oxide (TiO₂), aluminium, and polydimethylsiloxane (PDMS) as a microfluidic channel. The fabricated device achieved a LOD of 52nM utilizing I-V curves and a resistance ratio (Roff/Ron). Duwarah et al. [97] used zinc sulphide (ZnS) quantum dots nanostructures as memristor devices to detect *Escherichia coli* (*E. coli*) bacteria. The ZnS nano-sample was placed on top of an ITO glass substrate with a Cu electrode on top for the electrical characterization through the memristive voltage gap visible in the log of current vs voltage graphs at different concentrations of *E. coli*. Tzouvadaki et al. [20] fabricated a modified metal oxide memristor composed of titanium, titanium oxide, platinum, and aluminium oxide, all on top of a silicon wafer, used for the detection of PSA using chemical state variables. The memristor could detect a change in chemical state (antigen uptake) as a change in resistive state with the lowest detected PSA concentration of 0.6 ng/mL.

Studies on memristive biosensing are abundantly experimental, and very few utilize computations or modelling. Two of the few computational studies modelling memristive biosensors were conducted by Tzouvadaki et al. [98], [99]. The latter, more recent work of the two, demonstrated the electrical characterization of memristive nanowire sensors

before functionalization (bare sensor), after antibody functionalization, and during antigen uptake by modelling the sensor as an equivalent circuit for each stage. A summary of all published works on memristive biosensors highlighting their types, findings, and limitations are listed in Table 2.

B. FABRICATION OF SILICON NANOWIRES

Most current memristive studies utilized planar (horizontal) silicon nanowires to detect cancer biomarkers. This is due to the higher area-to-volume ratio of planar silicon nanowires compared to vertical standalone ones, which allows for accurate sensing of a minor change in the charge on the surface of such devices caused by the functionalization of antibodies and uptake of antigens. Due to this abundant usage of silicon nanowires in memristive biosensing, the different fabrication techniques of such structures are discussed in this subsection.

Silicon nanowires are fabricated through two techniques, namely, bottom-up and top-down approaches. The bottom-up approach uses a catalyst to direct the growth of nanowires on a substrate in a silicon-containing reactive environment. The most common growth process for bottom-up fabrication is vapour-liquid-solid (VLS), which results in meshes of nanowires in different configurations. The main drawback of this technique lies in the requirement of high-accuracy alignment processes for transferring the silicon nanowires onto the surface of the device where the electrodes are placed. This limits the standardization and capability of fabrication in the bulk of this technique. On the other hand, the top-down approach directly fabricates nanowires on the silicon device using E-beam or focused ion-beam lithography (FIB), which increases the standardization of the process.

C. OTHER TYPES OF BIOSENSING DEVICES

As mentioned, memristors started being implemented in various fields, including biosensing, in the past decade. Other biosensing devices based on the electrical characterization and detection of molecules, such as FETs and composite immunosensor electrodes, have been utilized for the same purpose. For example, Patolsky et al. [100] fabricated silicon nanowires covalently functionalized with anti-PSA antibodies to detect PSA under the working principle of FETs. The device utilized the change in conductance because of a change in the electric field or surface voltage when varying the concentration of PSA. In another study, Gao et al. [16] fabricated a graphene field-effect transistor to detect PSA. A covalent antibody attachment was used on the device, which allowed for the detection of PSA at a limit of 1 nM. An example of the second type of fabricated device is illustrated by the work of Jonous et al. [51]. They fabricated a sandwich electrode composed of reduced graphene oxide (rGO) and gold nanoparticles covalently functionalized with anti-total and anti-free PSA antibodies. The device utilized square wave and cyclic voltammetry for electrical characterization, resulting in a LOD of 0.2 ng/mL

TABLE 2. Summary of studies on memristive biosensors.

Ref.	Memristor Type	Analyte detected	Findings	Limitations
[18]	Si nanowires with NiSi contacts	Rabbit Antigen	<ul style="list-style-type: none"> • Memristive biosensors made of silicon nanowires are used to detect rabbit antigens with high sensitivity and LOD. • The effect of air humidity on the voltage gap of the sensor is investigated. 	<ul style="list-style-type: none"> • The reproducibility of biosensors is not indicated. • Biosensing of antigens is limited to pretreated solutions.
[89]	Multi-panel of 12 Si nanowires memristors with NiSi contacts	Rabbit and Prostate Specific Antigens	<ul style="list-style-type: none"> • Design and fabrication of multiple biosensors on a single chip demonstrating multi-panel sensing. • Demonstration of the individualized bio-functionalization of a particular nanostructure on a chip. • Detection of specific analytes in the presence of non-specific analytes. 	<ul style="list-style-type: none"> • Biosensing of antigens is limited to pretreated solutions.
[48, 49]	Si nanowires with NiSi contacts	VEGF	<ul style="list-style-type: none"> • High reproducibility was demonstrated by comparing the voltage gap of 20 memristors. • Investigation of an equivalent circuit model demonstrating the behaviour of a memristive biosensor. • Studied the effect of relative humidity on the voltage gap of the memristors. 	<ul style="list-style-type: none"> • Biosensing of VEGF is limited to pretreated solutions.
[47]	Si nanowires with NiSi contacts	PSA	<ul style="list-style-type: none"> • DNA aptamer-modified memristive biosensors are used for the detection of PSA. • Obtained a LOD of 23 aM, the lowest concentration published for PSA detection. • High reproducibility was demonstrated by comparing the voltage gap of 10 memristors. 	<ul style="list-style-type: none"> • Biosensing of PSA is limited to pretreated solutions.
[91, 92]	Si nanowires with NiSi contacts	PSA-IgM	<ul style="list-style-type: none"> • Utilizing the voltage gap of a memristive biosensor for the detection of PSA-IgM biomarker and comparison with the Enzyme-linked immunosorbent assay method (ELISA) through optical density. 	<ul style="list-style-type: none"> • High variation in fabricated devices due to the nature of the top-down fabrication technique utilized. • Biosensing of antigens is limited to pretreated solutions.
[45]	12 Si nanowires memristors with NiSi contacts placed on an electronic board prototype	PSA	<ul style="list-style-type: none"> • Design and fabrication of a biosensing board prototype consisting of a sensing module, microcontroller, data storage, and power supply. • Board is capable of sensing different biomarkers simultaneously. • The initial board prototype is a good candidate for point-of-care applications. 	<ul style="list-style-type: none"> • The reproducibility of biosensors is not indicated. • Biomarker detection results are at a proof-of-concept level.
[93]	Si nanowires with NiSi contacts	PSA	<ul style="list-style-type: none"> • Accurate detection of free PSA using silicon nanowire memristors. • Investigate the effect of antibody size on the memristor's voltage gap. The antibodies studied are anti-PSA single-chain antibody fragments, anti-PSA full-chain antibodies, and anti-PSA DNA-aptamers. 	<ul style="list-style-type: none"> • Inconsistent variation in the memristors' output (voltage gap) across different PSA concentrations. • Biosensing of antigens is limited to pretreated solutions.
[94]	Si nanowires with NiSi contacts	Tenofovir	<ul style="list-style-type: none"> • Sensitive detection of Tenofovir using memristive silicon nanowires functionalized with DNA aptamers. • Tenofovir is detected in both buffer and full human serum. 	<ul style="list-style-type: none"> • Low reproducibility is indicated by the high variation in voltage gap between the biosensors when detecting high concentrations of Tenofovir.
[50]	Honeycomb-shaped nanowires connected to source, drain, and reference	Ebola VP40 protein	<ul style="list-style-type: none"> • Detection of Ebola protein using the fabricated biosensor in both memristor and FET modes achieved better results than the traditional Enzyme-linked immunosorbent assay method (ELISA). 	<ul style="list-style-type: none"> • The reproducibility of biosensors is not indicated. • Biosensing of Ebola protein is limited to pretreated solutions.

TABLE 2. (Continued.) Summary of studies on memristive biosensors.

	electrodes composed of Ti and Ag layers.		<ul style="list-style-type: none"> Investigation of the bare biosensors' performance in pH sensing 	
[95, 96]	Glass/ITO/TiO ₂ /Al sandwich type in PDMS	NS1 protein	<ul style="list-style-type: none"> A microfluidic chamber was used to transport the sample onto the biosensor's bio-functionalized surface. NS1 protein concentrations are detected through a change in the Off-On resistance ratio of the device. 	<ul style="list-style-type: none"> Biosensing of NS1 protein is limited to pretreated solutions.
[97]	ITO/Cu/ZnS quantum dots	Escherichia coli (E.coli) bacteria.	<ul style="list-style-type: none"> ZnS quantum dots were utilized as memristive nanostructures to detect Escherichia coli (E. coli) bacteria. 	<ul style="list-style-type: none"> Biosensing of E. coli bacteria is limited to pretreated solutions.
[20]	Si/SiO ₂ /Ti/Pt/TiO ₂ /Al ₂ O ₃ /Pt	PSA	<ul style="list-style-type: none"> Fabrication of metal-insulator-metal memristor detecting concentrations of PSA as a function of the device's resistive state. 	<ul style="list-style-type: none"> The reproducibility of biosensors is not indicated. Biosensing of PSA is limited to pretreated solutions.
[98, 99]	Si nanowires	Rabbit antigens and VEGF	<ul style="list-style-type: none"> Developed a computational model mimicking the behaviour of memristive biosensors before functionalization, after functionalization, and after antigen uptake. The model is validated experimentally, showing good agreement. 	

Si: silicon, NiSi: nickel silicide, Ti: titanium, Ag: silver, ITO: indium tin oxide, TiO₂: titanium dioxide, Al: aluminium, PDMS:

polydimethylsiloxane, Cu: copper, ZnS: zinc sulphide, SiO₂: Silicon dioxide, Pt: platinum, Al₂O₃: Aluminum oxide, NS1: non-structural protein 1, VEGF: Vascular Endothelial Growth Factor

for total PSA and 0.07 ng/mL for free PSA, respectively. Wu et al. [52] fabricated a label-free device consisting of Au/Ag-rGO with added aminated and carboxyl graphene quantum dots functionalized with an anti-PSA antibody. The sensor used electrochemiluminescence (ECL) intensity to detect PSA at a 0.29 pg/mL limit.

A summary of all presented studies and more on the detection of various biomarkers using memristive sensors, field effect transistors (FETs), and composite immunosensor electrodes is included in Table 3. The table compares different types of biosensing devices that detect various biomarkers, highlighting biosensor type, the detected biomarker, type of antibody attachment, type of electrical characterization used, and LOD. Although this review focuses on the detection of cancer biomarkers like PSA, CEA, and VEGF, which were discussed in Section III-C, other studies conducted on non-cancer biomarkers have been discussed and summarized because of similarities in devices and working principles. These include studies on rabbit antigens, Ebola

VP40 matrix virus, non-structural protein 1 (NS1), tenofovir antiviral drug, Escherichia coli bacteria, and Avian Salmonellosis bacteria. For comparative reasons, the bold values of LOD in the table are converted from g/mL to the unit of Molarity or molar concentration (M) defined as mol/L, using the molar mass of the biomarker being detected. It is important to note that all the studies presented in Table 3 used in-vitro samples in which the detected biomarker was prepared in a serum solution. It is evident from the table that most of the studies presented utilized covalent attachment for antibody functionalization of the sensors. Moreover,

as indicated by the table, most works using memristor devices achieved a LOD in the fM range. In contrast, studies working with immunosensor electrodes attained a LOD in the pM range.

D. ADVANTAGES AND LIMITATIONS

Some advantages of traditional electrochemical biosensing devices like FETs are their high sensitivity to minute alterations in biological signals, low power consumption, and ease of microfluidic device integration. The other type of traditional devices, namely composite immunosensor electrodes offers advantages like high reproducibility and stability, cost reduction through simpler fabrication, and detection of multiple analytes simultaneously through multiplexing. One of the main limitations of FETs is the low sensing capability of high-ionic solutions due to the Debye screening effect [16]. This drawback is not noted in the case of memristive biosensing devices since they usually have a better active sensing region. Another advantage of memristors over traditional biosensing devices is the superior LOD achieved in most instances, where memristors achieve a LOD in the range of fM. In contrast, FETs and composite immunosensor electrode devices achieve a LOD in the pM and nM range.

The main limitation of memristive biosensors is the reproducibility of the fabricated devices. This limitation mainly arises from the inconsistency embedded in the fabrication technique of the sensor and during the antibody attachment process, where different amounts of antibody may functionalize on the surface. This increases the difficulty

TABLE 3. Comparison between different types of biosensors on the detection of several biomarkers.

Ref.	Biosensor Type	Biomarker detected	Antibody Attachment	Characterization technique	LOD	Sensitivity
[19]	Memristor SiNW	PSA	Direct adsorption	Memristive voltage gap	3.3 fM	-
[47]	Memristor SiNW	PSA	Affinity	Memristive voltage gap	23 aM	-
[18]	Memristor SiNW	Rabbit Antigens	Covalent (GPTS)	Memristive voltage gap	3.4±1.8 fM	37±1 mV/fM
[100]	FET SiNW	PSA	-	Conductance vs time curves	90 fg/mL or ~2.5 fM	-
[20]	Memristor	PSA	Direct adsorption	Resistance change	60.9 ng/mL ~ 1.69 nM	68.7±12.7 kΩ/[dec.C _{PSA}]
[50]	Memristor/FET	Ebola VP40 matrix protein	Covalent (EDC and NHS)	Memristive voltage gap	6 fM	50 mV/pH
[16]	FET	PSA	Covalent (EDC and NHS)	Conductance vs time curves	1 nM	0.152 mV/mM
[45, 46]	Memristor SiNW	VEGF	Covalent (GPTS)	Memristive voltage gap	0.6 to 2.1 fM	-
[95, 96]	Glass/ITO/TiO ₂ /Al/PDMS Memristor	NS1	Covalent (GPTS)	Memristive voltage gap and the off-on resistance ratio	52 nM	8.21×10 ⁻³ 1/nM
[97]	Glass/ZnS Quantum Dots Memristor	E. coli	-	Memristive voltage gap	-	-
[51]	rGO/AuNPs/anti-PSA antibody (sandwich)	PSA	Covalent (EDC and NHS)	SWV and CV	0.2 ng/mL ~ 5.55 pM and 0.07 ng/mL ~ 1.94 pM for total PSA and free PSA antigens, respectively.	-
[102]	rGO/G-C ₃ N ₄ /AuNPs/ aptamer	PSA	-	SWV and CV	1.67 pg/mL ~ 0.046 pM	-
[52]	Au/Ag-rGO/Aminated-GQDs/Carboxyl-GQDs	PSA	Covalent (EDC and NHS)	ECL intensity	0.29 pg/mL ~ 8.05 fM	-
[53]	GO/Fe ₃ O ₄ / PSA antibody	PSA	Covalent (EDC and NHS)	SWV and CV	15 fg/mL ~ 0.416 fM	0.0361 nA/log(pg/mL)
[54]	GCE/rGO/CEA antibody	CEA	Covalent (EDC and NHS)	CV and EIS	0.05 ng/mL ~ 0.277 pM	-
[17]	Graphene FET/CEA antibody	CEA	Non-Covalent	Source-drain voltage-current curves	100 pg/mL ~ 0.55 pM	-
[55]	FTO/rGO/antibody/Ag	Avian Salmonellosis	Covalent (EDC and NHS)	CV and DPV	25 and 37 cells of S.gal and S.pul.	-
[46]	GCE/3D Pt/HGO	CEA	Direct adsorption	CV and DPV	0.0006 ng/mL ~ 3.33 fM	5 μA/logC _{CEA} (ng/mL)
[103]	Graphene/PEDOT:PSS/Aptamer	CEA	-	EIS	0.45 ng/mL ~ 2.5 pM	-

SWV: Square wave voltammetry, CV: Cyclic Voltammetry, ECL: Electrochemiluminescence, EIS: Electrochemical impedance spectroscopy, DPV: differential pulse voltammetry

in reproducing sensors with identical sensing properties across different fabrication batches. One solution for such a challenge is using planar devices where multiple sensors are fabricated simultaneously in one fabrication step. This reduces the variation in the production of such sensors and increases uniformity. Another resolution when it comes to memristive sensors is altering the viscosity of the solution containing the sensor, which could enhance the reproducibility and stability of fabrication. Another disadvantage arises from the fact that all current memristive biosensors are silicon nanowires, which increases the complexity of fabrication and requires specialized equipment. This limitation may be eliminated by exploring different materials and structures that behave like memristors. Such an example could be the use of reduced graphene oxide as a memristor for detecting cancer biomarkers, as it has been shown to exhibit memristive features [101].

Finally, a significant limitation in most electrochemical biosensing devices, including memristors, that keeps them from being utilized clinically is the required pre-treatment of samples, for which devices capable of processing untreated human blood samples have not been developed. Most current electrochemical biosensing techniques can detect antigens in a pretreated solution. This leaves the current state of memristive and traditional electrochemical biosensors at a proof-of-concept level. The main limitation stopping such sensors from reaching promising clinical relevance and becoming a great candidate for point-of-care (PoC) devices clinically is the inability to selectively detect a particular analyte in a complex blood sample composed of numerous molecule types. However, suppose this limitation is overcome in the future. In that case, the proposed memristive biosensors can reduce the required screening time and offer an on-site detection of biomarkers, unlike current clinical detection assays which are run on big analyzers at specialized testing facilities, leading to a relatively slow screening process. A more advanced challenge would be the characterization and sensing of cancerous cells at the cell and subcellular levels. This opens the door to new challenges like the lysing of cells and the standardization of the conductivity of the solutions containing cells and sub-cells.

V. CONCLUSION AND REMARKS

In recent years, memristors have gained tremendous attention from researchers in various fields and applications. This paper reviews the different applications of memristors, the history of memristors, and the general working principle of memristors. More specifically, it looks deeply at the current studies where memristors are used as biosensors for cancer biomarker detection compared to other devices developed for the same application. The attachment of antibodies to the surface of a memristor results in a change in conductance, which appears as a change in voltage gap when compared to the bare device. However, when immersing the sensor in a solution containing target antigens, antibody-antigen interaction causes a masking effect on the change in voltage

gap, taking it back closer to the bare memristor case. From the review conducted, the LOD of memristive sensors appears to be, in most cases, better than that of other devices like FETs and immunosensor electrodes. Moreover, most fabricated memristive biosensors are composed of silicon nanowires. This calls for exploring different materials and structures to be used as memristive biosensing devices. Given its conductive properties and remarkable memristor behaviour, reduced graphene oxide could be a promising candidate. A vital recommendation for future research in this area is the exploration and design of memristive devices capable of handling actual blood samples, where the biosensing and characterization of cells and sub-cells would be possible. This objective raises challenges that currently do not exist, like controlling the conductivity of the cell's solution and the lysing of cells.

ETHICS APPROVAL AND CONSENT TO PARTICIPATE

All authors state that they adhere to the Ethical Responsibilities of Authors. In addition, this article does not contain any studies with human participants or animals performed by any of the authors.

CONSENT FOR PUBLICATION

All authors consent to the publication of the manuscript in journal of IEEE Access

DATA AVAILABILITY

All data generated or analyzed during this study are included in this published article.

COMPETING INTERESTS

The authors declare that there are no competing interests.

REFERENCES

- [1] A. Alazzam, B. Mathew, and F. Alhammadi, "Novel microfluidic device for the continuous separation of cancer cells using dielectrophoresis," *J. Separat. Sci.*, vol. 40, no. 5, pp. 1193–1200, Mar. 2017, doi: [10.1002/jssc.201601061](https://doi.org/10.1002/jssc.201601061).
- [2] F. Petersson, L. Åberg, A.-M. Swärd-Nilsson, and T. Laurell, "Free flow acoustophoresis: Microfluidic-based mode of particle and cell separation," *Anal. Chem.*, vol. 79, no. 14, pp. 5117–5123, Jul. 2007, doi: [10.1021/ac070444e](https://doi.org/10.1021/ac070444e).
- [3] N. Pamme and C. Wilhelm, "Continuous sorting of magnetic cells via on-chip free-flow magnetophoresis," *Lab Chip*, vol. 6, no. 8, p. 974, 2006, doi: [10.1039/b604542a](https://doi.org/10.1039/b604542a).
- [4] M. Ghorbanzadeh, M. K. Moravvej-Farshi, and S. Darbari, "Designing a plasmonic optophoresis system for trapping and simultaneous sorting/counting of micro- and nano-particles," *J. Lightw. Technol.*, vol. 33, no. 16, pp. 3453–3460, Aug. 15, 2015, doi: [10.1109/JLT.2015.2407408](https://doi.org/10.1109/JLT.2015.2407408).
- [5] S. Choi, S. Song, C. Choi, and J.-K. Park, "Continuous blood cell separation by hydrophoretic filtration," *Lab Chip*, vol. 7, no. 11, p. 1532, 2007, doi: [10.1039/b705203k](https://doi.org/10.1039/b705203k).
- [6] L. R. Huang, E. C. Cox, R. H. Austin, and J. C. Sturm, "Continuous particle separation through deterministic lateral displacement," *Science*, vol. 304, no. 5673, pp. 987–990, May 2004, doi: [10.1126/science.1094567](https://doi.org/10.1126/science.1094567).
- [7] S. Kumar, Z. Wang, W. Zhang, X. Liu, M. Li, G. Li, B. Zhang, and R. Singh, "Optically active nanomaterials and its biosensing applications—A review," *Biosensors*, vol. 13, no. 1, p. 85, Jan. 2023, doi: [10.3390/BIOS13010085](https://doi.org/10.3390/BIOS13010085).

- [8] U. Chadha, P. Bhardwaj, R. Agarwal, P. Rawat, R. Agarwal, I. Gupta, M. Panjwani, S. Singh, C. Ahuja, S. K. Selvaraj, M. Banavoth, P. Sonar, B. Badoni, and A. Chakravorty, "Recent progress and growth in biosensors technology: A critical review," *J. Ind. Eng. Chem.*, vol. 109, pp. 21–51, May 2022, doi: [10.1016/j.jiec.2022.02.010](https://doi.org/10.1016/j.jiec.2022.02.010).
- [9] A. K. Pathak and C. Vipavakit, "A review on all-optical fiber-based VOC sensors: Heading towards the development of promising technology," *Sens. Actuators A, Phys.*, vol. 338, May 2022, Art. no. 113455, doi: [10.1016/j.sna.2022.113455](https://doi.org/10.1016/j.sna.2022.113455).
- [10] I. Novodchuk, M. Bajcsy, and M. Yavuz, "Graphene-based field effect transistor biosensors for breast cancer detection: A review on biosensing strategies," *Carbon*, vol. 172, pp. 431–453, Feb. 2021, doi: [10.1016/j.carbon.2020.10.048](https://doi.org/10.1016/j.carbon.2020.10.048).
- [11] C. Ricciardi, I. Ferrante, R. Castagna, F. Frascella, S. L. Marasso, K. Santoro, M. Gili, D. Pitardi, M. Pezzolato, and E. Bozzetta, "Immunodetection of 17 β -estradiol in serum at ppt level by microcantilever resonators," *Biosensors Bioelectron.*, vol. 40, no. 1, pp. 407–411, Feb. 2013, doi: [10.1016/j.bios.2012.08.043](https://doi.org/10.1016/j.bios.2012.08.043).
- [12] A. J. Haes, L. Chang, W. L. Klein, and R. P. Van Duyne, "Detection of a biomarker for Alzheimer's disease from synthetic and clinical samples using a nanoscale optical biosensor," *J. Amer. Chem. Soc.*, vol. 127, no. 7, pp. 2264–2271, Feb. 2005, doi: [10.1021/ja044087q](https://doi.org/10.1021/ja044087q).
- [13] Y. Deng, W. Wang, L. Zhang, Z. Lu, S. Li, and L. Xu, "Preparation and electrochemical behavior of L-glutamate electrochemical biosensor," *J. Biomed. Nanotechnol.*, vol. 9, no. 2, pp. 318–321, Feb. 2013, doi: [10.1166/jbn.2013.1487](https://doi.org/10.1166/jbn.2013.1487).
- [14] M. A. Nahid, C. E. Campbell, K. S. K. Fong, J. C. Barnhill, and M. A. Washington, "An evaluation of the impact of clinical bacterial isolates on epithelial cell monolayer integrity by the electric cell-substrate impedance sensing (ECIS) method," *J. Microbiol. Methods*, vol. 169, Feb. 2020, Art. no. 105833, doi: [10.1016/j.mimet.2020.105833](https://doi.org/10.1016/j.mimet.2020.105833).
- [15] F. Patolsky, G. Zheng, O. Hayden, M. Lakadamyali, X. Zhuang, and C. M. Lieber, "Electrical detection of single viruses," *Proc. Nat. Acad. Sci. USA*, vol. 101, no. 39, pp. 14017–14022, 2004. [Online]. Available: <http://www.pnas.org/cgi/doi/10.1073/pnas.0406159101>
- [16] N. Gao, T. Gao, X. Yang, X. Dai, W. Zhou, A. Zhang, and C. M. Lieber, "Specific detection of biomolecules in physiological solutions using graphene transistor biosensors," *Proc. Nat. Acad. Sci. USA*, vol. 113, no. 51, pp. 14633–14638, Dec. 2016, doi: [10.1073/pnas.1625010114](https://doi.org/10.1073/pnas.1625010114).
- [17] L. Zhou, H. Mao, C. Wu, L. Tang, Z. Wu, H. Sun, H. Zhang, H. Zhou, C. Jia, Q. Jin, X. Chen, and J. Zhao, "Label-free graphene biosensor targeting cancer molecules based on non-covalent modification," *Biosensors Bioelectron.*, vol. 87, pp. 701–707, Jan. 2017, doi: [10.1016/j.bios.2016.09.025](https://doi.org/10.1016/j.bios.2016.09.025).
- [18] S. Carrara, D. Sacchetto, M.-A. Doucey, C. Baj-Rossi, G. De Micheli, and Y. Leblebici, "Memristive-biosensors: A new detection method by using nanofabricated memristors," *Sens. Actuators B, Chem.*, vols. 171–172, pp. 449–457, Aug./Sep. 2012, doi: [10.1016/j.snb.2012.04.089](https://doi.org/10.1016/j.snb.2012.04.089).
- [19] Z. Zhao, S. Wang, S. Wang, X. Zhang, S. Ma, and J. Yang, "CNN-based bi-directional motion compensation for high efficiency video coding," in *Proc. IEEE Int. Symp. Circuits Syst. (ISCAS)*, May 2018, pp. 1–4.
- [20] I. Tzouvadaki, S. Stathopoulos, T. Abbey, L. Michalas, and T. Prodromakis, "Monitoring PSA levels as chemical state-variables in metal-oxide memristors," *Sci. Rep.*, vol. 10, no. 1, p. 15281, Sep. 2020, doi: [10.1038/s41598-020-71962-3](https://doi.org/10.1038/s41598-020-71962-3).
- [21] S. Carrara, "The birth of a new field: Memristive sensors. A review," *IEEE Sensors J.*, vol. 21, no. 11, pp. 12370–12378, Jun. 2021, doi: [10.1109/JSEN.2020.3043305](https://doi.org/10.1109/JSEN.2020.3043305).
- [22] L. O. Chua, "Memristor—The missing circuit element," *IEEE Trans. Circuit Theory*, vol. CT-18, no. 5, pp. 507–519, Sep. 1971, doi: [10.1109/TCT.1971.1083337](https://doi.org/10.1109/TCT.1971.1083337).
- [23] T. Prodromakis, "Two centuries of memristors," in *Chaos, CNN, Memristors and Beyond: A Festschrift for Leon Chua*. Singapore: World Scientific, 2013, doi: [10.1142/9789814434805_0041](https://doi.org/10.1142/9789814434805_0041).
- [24] D. B. Strukov, G. S. Snider, D. R. Stewart, and R. S. Williams, "The missing memristor found," *Nature*, vol. 453, no. 7191, pp. 80–83, May 2008, doi: [10.1038/nature06932](https://doi.org/10.1038/nature06932).
- [25] M. Naqi, M. S. Kang, N. Liu, T. Kim, S. Baek, A. Bala, C. Moon, J. Park, and S. Kim, "Multilevel artificial electronic synaptic device of direct grown robust MoS₂ based memristor array for in-memory deep neural network," *npj 2D Mater. Appl.*, vol. 6, no. 1, p. 53, Aug. 2022, doi: [10.1038/s41699-022-00325-5](https://doi.org/10.1038/s41699-022-00325-5).
- [26] H. Ren, Z. Peng, and Y. Gu, "Fixed-time synchronization of stochastic memristor-based neural networks with adaptive control," *Neural Netw.*, vol. 130, pp. 165–175, Oct. 2020, doi: [10.1016/j.neunet.2020.07.002](https://doi.org/10.1016/j.neunet.2020.07.002).
- [27] R. V. Aravind and P. Balasubramaniam, "Stability criteria for memristor-based delayed fractional-order Cohen–Grossberg neural networks with uncertainties," *J. Comput. Appl. Math.*, vol. 420, Mar. 2023, Art. no. 114764, doi: [10.1016/j.cam.2022.114764](https://doi.org/10.1016/j.cam.2022.114764).
- [28] X.-W. Zhang, H.-N. Wu, J.-L. Wang, Z. Liu, and R. Li, "Membership-function-dependent fuzzy control of reaction-diffusion memristive neural networks with a finite number of actuators and sensors," *Neurocomputing*, vol. 514, pp. 94–100, Dec. 2022, doi: [10.1016/j.neucom.2022.09.126](https://doi.org/10.1016/j.neucom.2022.09.126).
- [29] L. Liu, Y. Wang, W. Chen, S. Ren, J. Guo, X. Kang, and X. Zhao, "Robust resistive switching in MoS₂-based memristor with Ti top electrode," *Appl. Surf. Sci.*, vol. 603, Dec. 2022, Art. no. 154698, doi: [10.1016/j.apsusc.2022.154698](https://doi.org/10.1016/j.apsusc.2022.154698).
- [30] J. Park, E. Park, and H.-Y. Yu, "Active layer nitrogen doping technique with excellent thermal stability for resistive switching memristor," *Appl. Surf. Sci.*, vol. 603, Nov. 2022, Art. no. 154307, doi: [10.1016/j.apsusc.2022.154307](https://doi.org/10.1016/j.apsusc.2022.154307).
- [31] Y. Deng, X. Xu, L. Zhang, F. Du, Q. Liu, J. Chen, K. Meng, Y. Wu, M. Yang, and Y. Jiang, "Lithium incorporation enhanced resistive switching behaviors in lithium lanthanum titanium oxide-based heterostructure," *J. Mater. Sci. Technol.*, vol. 128, pp. 142–147, Nov. 2022, doi: [10.1016/j.jmst.2022.04.029](https://doi.org/10.1016/j.jmst.2022.04.029).
- [32] S. Mao, B. Sun, Y. Yang, J. Wang, H. Zhao, and Y. Zhao, " α -MnO₂ nanorods-based memristors with nonvolatile resistive switching behavior," *Ceram. Int.*, vol. 48, no. 22, pp. 32860–32866, Nov. 2022, doi: [10.1016/j.ceramint.2022.07.213](https://doi.org/10.1016/j.ceramint.2022.07.213).
- [33] Q. Guo, N. Wang, and G. Zhang, "A novel four-element RCLM hyperchaotic circuit based on current-controlled extended memristor," *AEU-Int. J. Electron. Commun.*, vol. 156, Nov. 2022, Art. no. 154391, doi: [10.1016/j.aeue.2022.154391](https://doi.org/10.1016/j.aeue.2022.154391).
- [34] C. Hu, Z. Tian, Q. Wang, X. Zhang, B. Liang, C. Jian, and X. Wu, "A memristor-based VB2 chaotic system: Dynamical analysis, circuit implementation, and image encryption," *Optik*, vol. 269, Nov. 2022, Art. no. 169878, doi: [10.1016/j.jlleo.2022.169878](https://doi.org/10.1016/j.jlleo.2022.169878).
- [35] F. Setoudeh, M. M. Dezhdar, and M. Najafi, "Nonlinear analysis and chaos synchronization of a memristive-based chaotic system using adaptive control technique in noisy environments," *Chaos, Solitons Fractals*, vol. 164, Nov. 2022, Art. no. 112710, doi: [10.1016/j.chaos.2022.112710](https://doi.org/10.1016/j.chaos.2022.112710).
- [36] Q. Lai, L. Yang, and Y. Liu, "Design and realization of discrete memristive hyperchaotic map with application in image encryption," *Chaos, Solitons Fractals*, vol. 165, Dec. 2022, Art. no. 112781, doi: [10.1016/j.chaos.2022.112781](https://doi.org/10.1016/j.chaos.2022.112781).
- [37] X. Wang, Y. Chen, Y. Gu, and H. Li, "Spintronic memristor temperature sensor," *IEEE Electron Device Lett.*, vol. 31, no. 1, pp. 20–22, Jan. 2010, doi: [10.1109/LED.2009.2035643](https://doi.org/10.1109/LED.2009.2035643).
- [38] C. Jiang, Q. Li, N. Sun, J. Huang, R. Ji, S. Bi, Q. Guo, and J. Song, "A high-performance bionic pressure memory device based on piezo-OLED and piezo-memristor as luminescence-fish neuromorphic tactile system," *Nano Energy*, vol. 77, Nov. 2020, Art. no. 105120, doi: [10.1016/j.nanoen.2020.105120](https://doi.org/10.1016/j.nanoen.2020.105120).
- [39] H. Abunahla, B. Mohammad, L. Mahmoud, M. Darweesh, M. Alhawari, M. A. Jaoude, and G. W. Hitt, "MemSens: Memristor-based radiation sensor," *IEEE Sensors J.*, vol. 18, no. 8, pp. 3198–3205, Apr. 2018, doi: [10.1109/JSEN.2018.2808285](https://doi.org/10.1109/JSEN.2018.2808285).
- [40] M. Vidiš, T. Plecenik, M. Moško, S. Tomašec, T. Roch, L. Satrapinskyy, B. Grančič, and A. Plecenik, "Gasistor: A memristor based gas-triggered switch and gas sensor with memory," *Appl. Phys. Lett.*, vol. 115, no. 9, Aug. 2019, Art. no. 093504, doi: [10.1063/1.5099685](https://doi.org/10.1063/1.5099685).
- [41] M. C. Lemme, D. Akinwande, C. Huyghebaert, and C. Stampfer, "2D materials for future heterogeneous electronics," *Nature Commun.*, vol. 13, no. 1, Mar. 2022, doi: [10.1038/s41467-022-29001-4](https://doi.org/10.1038/s41467-022-29001-4).
- [42] K. S. Woo, J. Kim, J. Han, W. Kim, Y. H. Jang, and C. S. Hwang, "Probabilistic computing using Cu_{0.1}Te_{0.9}/HfO₂/Pt diffusive memristors," *Nature Commun.*, vol. 13, no. 1, p. 5762, Sep. 2022, doi: [10.1038/s41467-022-33455-x](https://doi.org/10.1038/s41467-022-33455-x).
- [43] A. Banerjee, A. Ghosh, M. Das, S. K. Suman, and A. Sain, "Memristor-based multiplier and squarer of some numbers of the form $10^l \pm m$," *J. Inst. Eng., India, B*, vol. 103, no. 4, pp. 1239–1247, Aug. 2022, doi: [10.1007/s40031-022-00717-7](https://doi.org/10.1007/s40031-022-00717-7).

- [44] M. Selmi and H. Belmabrouk, "AC electroosmosis effect on microfluidic heterogeneous immunoassay efficiency," *Micromachines*, vol. 11, no. 4, p. 342, Mar. 2020, doi: [10.3390/MII1040342](https://doi.org/10.3390/MII1040342).
- [45] *IEEE International Symposium on Circuits and Systems (ISCAS)*, IEEE, Piscataway, NJ, USA, 2018.
- [46] A. Jing, Q. Xu, W. Feng, and G. Liang, "An electrochemical immunosensor for sensitive detection of the tumor marker carcinoembryonic antigen (CEA) based on three-dimensional porous nanoplatinum/graphene," *Micromachines*, vol. 11, no. 7, p. 660, Jul. 2020, doi: [10.3390/mi11070660](https://doi.org/10.3390/mi11070660).
- [47] I. Tzouvadaki, P. Jolly, X. Lu, S. Ingebrandt, G. De Micheli, P. Estrela, and S. Carrara, "Label-free ultrasensitive memristive aptasensor," *Nano Lett.*, vol. 16, no. 7, pp. 4472–4476, Jul. 2016, doi: [10.1021/acs.nanolett.6b01648](https://doi.org/10.1021/acs.nanolett.6b01648).
- [48] F. Puppo, A. Dave, M.-A. Doucey, D. Sacchetto, C. Baj-Rossi, Y. Leblebici, G. De Micheli, and S. Carrara, "Memristive biosensors under varying humidity conditions," *IEEE Trans. Nanobiosci.*, vol. 13, no. 1, pp. 19–30, Mar. 2014, doi: [10.1109/TNB.2013.2295517](https://doi.org/10.1109/TNB.2013.2295517).
- [49] F. Puppo, M.-A. Doucey, M. Di Ventra, G. De Micheli, and S. Carrara, "Memristor-based devices for sensing," in *Proc. IEEE Int. Symp. Circuits Syst. (ISCAS)*, Melbourne, VIC, Australia, Jun. 2014, pp. 1–5, doi: [10.1109/ISCAS.2014.6865620](https://doi.org/10.1109/ISCAS.2014.6865620).
- [50] B. Ibarlucea, T. F. Akbar, K. Kim, T. Rim, C.-K. Baek, A. Ascoli, R. Tetzlaff, L. Baraban, and G. Cuniberti, "Ultrasensitive detection of Ebola matrix protein in a memristor mode," *Nano Res.*, vol. 11, no. 2, pp. 1057–1068, Feb. 2018, doi: [10.1007/s12274-017-1720-2](https://doi.org/10.1007/s12274-017-1720-2).
- [51] Z. A. Jonous, J. S. Shayeh, F. Yazdian, A. Yadegari, M. Hashemi, and M. Omid, "An electrochemical biosensor for prostate cancer biomarker detection using graphene oxide-gold nanostructures," *Eng. Life Sci.*, vol. 19, no. 3, pp. 206–216, Mar. 2019, doi: [10.1002/elsc.201800093](https://doi.org/10.1002/elsc.201800093).
- [52] D. Wu, Y. Liu, Y. Wang, L. Hu, H. Ma, G. Wang, and Q. Wei, "Label-free electrochemiluminescent immunosensor for detection of prostate specific antigen based on aminated graphene quantum dots and carboxyl graphene quantum dots," *Sci. Rep.*, vol. 6, no. 1, p. 20511, Feb. 2016, doi: [10.1038/srep20511](https://doi.org/10.1038/srep20511).
- [53] M. Sharafeldin, G. W. Bishop, S. Bhakta, A. El-Sawy, S. L. Suib, and J. F. Rusling, "Fe₃O₄ nanoparticles on graphene oxide sheets for isolation and ultrasensitive amperometric detection of cancer biomarker proteins," *Biosensors Bioelectron.*, vol. 91, pp. 359–366, May 2017, doi: [10.1016/j.bios.2016.12.052](https://doi.org/10.1016/j.bios.2016.12.052).
- [54] M. Jozghorbani, M. Fathi, S. H. Kazemi, and N. Alinejadani, "Determination of carcinoembryonic antigen as a tumor marker using a novel graphene-based label-free electrochemical immunosensor," *Anal. Biochem.*, vol. 613, Jan. 2021, Art. no. 114017, doi: [10.1016/j.ab.2020.114017](https://doi.org/10.1016/j.ab.2020.114017).
- [55] S. Mahari and S. Gandhi, "Electrochemical immunosensor for detection of avian Salmonellosis based on electroactive reduced graphene oxide (rGO) modified electrode," *Bioelectrochemistry*, vol. 144, Apr. 2022, Art. no. 108036, doi: [10.1016/j.bioelechem.2021.108036](https://doi.org/10.1016/j.bioelechem.2021.108036).
- [56] I. Tzouvadaki, N. Madaboosi, I. Taurino, V. Chu, J. P. Conde, G. De Micheli, and S. Carrara, "Study on the bio-functionalization of memristive nanowires for optimum memristive biosensors," *J. Mater. Chem. B*, vol. 4, no. 12, pp. 2153–2162, Mar. 2016, doi: [10.1039/c6tb00222f](https://doi.org/10.1039/c6tb00222f).
- [57] F. Ambrosetti, B. Jiménez-García, J. Roel-Touris, and A. M. J. J. Bonvin, "Modeling antibody-antigen complexes by information-driven docking," *Structure*, vol. 28, no. 1, pp. 119–129, Jan. 2020, doi: [10.1016/j.str.2019.10.011](https://doi.org/10.1016/j.str.2019.10.011).
- [58] E. J. Sundberg and R. A. Mariuzza, "Molecular recognition in antibody-antigen complexes," *Adv. Protein Chem.*, vol. 61, pp. 119–160, Jan. 2002, doi: [10.1016/S0065-3233\(02\)61004-6](https://doi.org/10.1016/S0065-3233(02)61004-6).
- [59] A. Singh, A. Mishra, and A. Verma, "Antibodies: Monoclonal and polyclonal," in *Animal Biotechnology: Models in Discovery and Translation*. Cambridge, MA, USA: Academic, 2020, doi: [10.1016/B978-0-12-811710-1.00015-X](https://doi.org/10.1016/B978-0-12-811710-1.00015-X).
- [60] P. N. Nelson, "Demystified: Monoclonal antibodies," *Mol. Pathol.*, vol. 53, no. 3, pp. 111–117, Jun. 2000, doi: [10.1136/mp.53.3.111](https://doi.org/10.1136/mp.53.3.111).
- [61] G. Veggiani, J. Zuin, L. Beneduce, A. Gallotta, P. Pengo, and G. Fassina, "Combinatorial semisynthesis of biomarker-IgM complexes," *SLAS Discovery*, vol. 15, no. 10, pp. 1274–1280, Dec. 2010, doi: [10.1177/1087057110378623](https://doi.org/10.1177/1087057110378623).
- [62] M. Ezeani, C. Onyenekwe, S. Chukwuemeka, M. C. Ezeani, C. C. Onyenekwe, and S. C. Meludu, "Persistent circulating immune complexes: Potential source of epimutation and cancer poor prognosis," *Int. J. Genet. Genomics*, vol. 5, no. 1, pp. 1–13, 2017, doi: [10.11648/j.ijgg.20170501.11](https://doi.org/10.11648/j.ijgg.20170501.11).
- [63] L. Beneduce, T. Prayer-Galetti, A. M. G. Giustinian, A. Gallotta, G. Betto, F. Pagano, and G. Fassina, "Detection of prostate-specific antigen coupled to immunoglobulin m in prostate cancer patients," *Cancer Detection Prevention*, vol. 31, no. 5, pp. 402–407, Jan. 2007, doi: [10.1016/j.cdp.2007.10.005](https://doi.org/10.1016/j.cdp.2007.10.005).
- [64] F. Castaldi, M. Marino, L. Beneduce, C. Belluco, F. De Marchi, E. Mammano, D. Nitti, M. Lise, and G. Fassina, "Detection of circulating CEA-IgM complexes in early stage colorectal cancer," *Int. J. Biol. Markers*, vol. 20, no. 4, pp. 204–208, Oct. 2005, doi: [10.1177/172460080502000402](https://doi.org/10.1177/172460080502000402).
- [65] P. Pontisso, S. Quarta, C. Caberlotto, L. Beneduce, M. Marino, E. Bernardinello, N. Tono, G. Fassina, L. Cavalletto, A. Gatta, and L. Chemello, "Progressive increase of SCCA-IgM immune complexes in cirrhotic patients is associated with development of hepatocellular carcinoma," *Int. J. Cancer*, vol. 119, no. 4, pp. 735–740, Aug. 2006, doi: [10.1002/ijc.21908](https://doi.org/10.1002/ijc.21908).
- [66] L. Beneduce, F. Castaldi, M. Marino, N. Tono, A. Gatta, P. Pontisso, and G. Fassina, "Improvement of liver cancer detection with simultaneous assessment of circulating levels of free alpha-fetoprotein (AFP) and AFP-IgM complexes," *Int. J. Biol. Markers*, vol. 19, no. 2, pp. 155–159, Apr. 2004, doi: [10.1177/172460080401900211](https://doi.org/10.1177/172460080401900211).
- [67] H. B. Huu, N. H. Thuc, H. P. T. Le, T. D. T. Thanh, A. L. Bac, C. Tiribelli, P. Pontisso, A. Gallotta, L. Paneghetti, and G. Fassina, "Characterization of SCCA-IgM as a biomarker of liver disease in an Asian cohort of patients," *Scandin. J. Clin. Lab. Invest.*, vol. 78, no. 3, pp. 204–210, Apr. 2018, doi: [10.1080/00365513.2018.1432072](https://doi.org/10.1080/00365513.2018.1432072).
- [68] L. Beneduce, G. Pesce, A. Gallotta, F. Zampieri, A. Biasiolo, N. Tono, N. Boscato, A. Gatta, P. Pontisso, and G. Fassina, "Tumour-specific induction of immune complexes: DCP-IgM in hepatocellular carcinoma," *Eur. J. Clin. Invest.*, vol. 38, no. 8, pp. 571–577, Aug. 2008, doi: [10.1111/j.1365-2362.2008.01985.x](https://doi.org/10.1111/j.1365-2362.2008.01985.x).
- [69] J. Zhang, G. Chen, P. Zhang, J. Zhang, X. Li, D. Gan, X. Cao, M. Han, H. Du, and Y. Ye, "The threshold of alpha-fetoprotein (AFP) for the diagnosis of hepatocellular carcinoma: A systematic review and meta-analysis," *PLoS ONE*, vol. 15, no. 2, Feb. 2020, Art. no. e0228857, doi: [10.1371/JOURNAL.PONE.0228857](https://doi.org/10.1371/JOURNAL.PONE.0228857).
- [70] M. Cagnin, A. Biasiolo, A. Martini, M. Ruvoletto, S. Quarta, S. Fasolato, P. Angeli, G. Fassina, and P. Pontisso, "Serum squamous cell carcinoma antigen-immunoglobulin M complex levels predict survival in patients with cirrhosis," *Sci. Rep.*, vol. 9, no. 1, pp. 1–8, Dec. 2019, doi: [10.1038/s41598-019-56633-2](https://doi.org/10.1038/s41598-019-56633-2).
- [71] M. Grunnet and J. B. Sorensen, "Carcinoembryonic antigen (CEA) as tumor marker in lung cancer," *Lung Cancer*, vol. 76, no. 2, pp. 138–143, May 2012, doi: [10.1016/j.lungcan.2011.11.012](https://doi.org/10.1016/j.lungcan.2011.11.012).
- [72] S. Tang, F. Zhou, Y. Sun, L. Wei, S. Zhu, R. Yang, Y. Huang, and J. Yang, "CEA in breast ductal secretions as a promising biomarker for the diagnosis of breast cancer: A systematic review and meta-analysis," *Breast Cancer*, vol. 23, no. 6, pp. 813–819, Nov. 2016.
- [73] A. K. Pandey, E. K. Singhi, J. P. Arroyo, T. A. Ikizler, E. R. Gould, J. Brown, J. A. Beckman, D. G. Harrison, and J. Moslehi, "Mechanisms of VEGF (vascular endothelial growth factor) inhibitor-associated hypertension and vascular disease," *Hypertension*, vol. 71, no. 2, pp. e1–e8, Feb. 2018, doi: [10.1161/HYPERTENSIONAHA.117.10271](https://doi.org/10.1161/HYPERTENSIONAHA.117.10271).
- [74] K. B. Neves, F. J. Rios, L. van der Mey, R. Alves-Lopes, A. C. Cameron, M. Volpe, A. C. Montezano, C. Savoia, and R. M. Touyz, "VEGFR (vascular endothelial growth factor receptor) inhibition induces cardiovascular damage via redox-sensitive processes," *Hypertension*, vol. 71, no. 4, pp. 638–647, Apr. 2018, doi: [10.1161/HYPERTENSION-AHA.117.10490](https://doi.org/10.1161/HYPERTENSION-AHA.117.10490).
- [75] M. K. Sezgentürk, "A new impedimetric biosensor utilizing VEGF receptor-1 (Flt-1): Early diagnosis of vascular endothelial growth factor in breast cancer," *Biosensors Bioelectron.*, vol. 26, no. 10, pp. 4032–4039, Jun. 2011, doi: [10.1016/j.bios.2011.03.025](https://doi.org/10.1016/j.bios.2011.03.025).
- [76] M. Akgün and M. K. Sezgentürk, "A novel biosensing system based on ITO-single use electrode for highly sensitive analysis of VEGF," *Int. J. Environ. Anal. Chem.*, vol. 100, no. 4, pp. 432–450, Mar. 2020, doi: [10.1080/03067319.2019.1709637](https://doi.org/10.1080/03067319.2019.1709637).
- [77] A. T. Baron, C. H. Boardman, J. M. Lafky, A. Rademaker, D. Liu, D. A. Fishman, K. C. Podratz, and N. J. Maithe, "Soluble epidermal growth factor receptor (SEG-FR) and cancer antigen 125 (CA125) as screening and diagnostic tests for epithelial ovarian cancer," *Cancer Epidemiol., Biomarkers Prevention*, vol. 14, no. 2, pp. 306–318, Feb. 2005, doi: [10.1158/1055-9965.EPI-04-0423](https://doi.org/10.1158/1055-9965.EPI-04-0423).

- [78] P. Charkhchi, C. Cybulski, J. Gronwald, F. O. Wong, S. A. Narod, and M. R. Akbari, "CA125 and ovarian cancer: A comprehensive review," *Cancers*, vol. 12, no. 12, p. 3730, Dec. 2020, doi: [10.3390/CANCERS12123730](https://doi.org/10.3390/CANCERS12123730).
- [79] Y. Tang, Y. Cui, S. Zhang, and L. Zhang, "The sensitivity and specificity of serum glycan-based biomarkers for cancer detection," *Prog. Mol. Biol. Transl. Sci.*, vol. 162, pp. 121–140, 2019, doi: [10.1016/BS.PMBTS.2019.01.010](https://doi.org/10.1016/BS.PMBTS.2019.01.010).
- [80] G. Funston, W. Hamilton, G. Abel, E. J. Crosbie, B. Rous, and F. M. Walter, "The diagnostic performance of CA125 for the detection of ovarian and non-ovarian cancer in primary care: A population-based cohort study," *PLOS Med.*, vol. 17, no. 10, Oct. 2020, Art. no. e1003295, doi: [10.1371/JOURNAL.PMED.1003295](https://doi.org/10.1371/JOURNAL.PMED.1003295).
- [81] R. Lombardo, G. Tema, F. Cancrini, L. Albanesi, L. Mavilla, P. Taricotti, B. C. Gentile, P. Aloisi, G. Rizzo, S. Tardioli, and R. Giulianelli, "The role of immune PSA complex (iXip) in the prediction of prostate cancer," *Biomarkers*, vol. 26, no. 1, pp. 26–30, Jan. 2021, doi: [10.1080/1354750X.2020.1841294](https://doi.org/10.1080/1354750X.2020.1841294).
- [82] J. S. Kim, J.-G. Ryu, J. W. Kim, E. C. Hwang, S. I. Jung, T. W. Kang, D. Kwon, and K. Park, "Prostate-specific antigen fluctuation: What does it mean in diagnosis of prostate cancer?" *Int. Brazilian J. Urol.*, vol. 41, no. 2, pp. 258–264, Apr. 2015, doi: [10.1590/S1677-5538.IBJU.2015.02.11](https://doi.org/10.1590/S1677-5538.IBJU.2015.02.11).
- [83] I. M. Thompson, D. P. Ankerst, C. Chi, M. S. Lucia, P. J. Goodman, J. J. Crowley, H. L. Parnes, and C. A. Coltman, "Operating characteristics of prostate-specific antigen in men with an initial PSA level of 3.0 ng/mL or lower," *JAMA*, vol. 294, no. 1, pp. 66–70, Jul. 2005, doi: [10.1001/JAMA.294.1.66](https://doi.org/10.1001/JAMA.294.1.66).
- [84] D. Zani, S. Costa, L. Beneduce, G. Fassina, C. Simeone, and S. C. Cunico, "Immunity and cancer: The role of PSA IgM immune complexes for prostate cancer," *Urologia J.*, vol. 77, no. 1, pp. 1–3, Jan. 2010, doi: [10.1177/039156031007700101](https://doi.org/10.1177/039156031007700101).
- [85] D. A. Healy, C. J. Hayes, P. Leonard, L. McKenna, and R. O'Kennedy, "Biosensor developments: Application to prostate-specific antigen detection," *Trends Biotechnol.*, vol. 25, no. 3, pp. 125–131, Mar. 2007, doi: [10.1016/j.tibtech.2007.01.004](https://doi.org/10.1016/j.tibtech.2007.01.004).
- [86] H. Akiba and K. Tsumoto, "Thermodynamics of antibody–antigen interaction revealed by mutation analysis of antibody variable regions," *J. Biochem.*, vol. 158, no. 1, pp. 1–13, Jul. 2015, doi: [10.1093/jb/mvv049](https://doi.org/10.1093/jb/mvv049).
- [87] C. J. van Oss, "Antibody–antigen intermolecular forces," in *Encyclopedia of Immunology*. Amsterdam, The Netherlands: Elsevier, Jan. 1998, pp. 163–167, doi: [10.1006/RWEI.1999.0045](https://doi.org/10.1006/RWEI.1999.0045).
- [88] M. H. V. V. Regenmortel, "Thermodynamic parameters in immunoassay," *Clin. Chem. Lab. Med.*, vol. 36, no. 6, pp. 353–354, Jun. 1998, doi: [10.1515/CCLM.1998.059](https://doi.org/10.1515/CCLM.1998.059).
- [89] I. Tzouvadaki, A. Tuoheti, S. Lorrain, M. Quadroni, M.-A. Doucey, G. De Micheli, D. Demarchi, and S. Carrara, "Multi-panel, on-single-chip memristive biosensing," *IEEE Sensors J.*, vol. 19, no. 14, pp. 5769–5774, Jul. 2019, doi: [10.1109/JSEN.2019.2904393](https://doi.org/10.1109/JSEN.2019.2904393).
- [90] M.-A. Doucey and S. Carrara, "Nanowire sensors in cancer," *Trends Biotechnol.*, vol. 37, no. 1, pp. 86–99, Jan. 2019, doi: [10.1016/j.tibtech.2018.07.014](https://doi.org/10.1016/j.tibtech.2018.07.014).
- [91] I. Tzouvadaki, X. Lu, G. De Micheli, S. Ingebrandt, and S. Carrara, "Nano-fabricated memristive biosensors for biomedical applications with liquid and dried samples," in *Proc. 38th Annu. Int. Conf. IEEE Eng. Med. Biol. Soc. (EMBC)*, Aug. 2016, pp. 295–298, doi: [10.1109/EMBC.2016.7590698](https://doi.org/10.1109/EMBC.2016.7590698).
- [92] I. Tzouvadaki, C. Parrozzani, A. Gallotta, G. De Micheli, and S. Carrara, "Memristive biosensors for PSA-IgM detection," *BioNanoScience*, vol. 5, no. 4, pp. 189–195, Oct. 2015, doi: [10.1007/s12668-015-0179-4](https://doi.org/10.1007/s12668-015-0179-4).
- [93] I. Tzouvadaki, J. Zapatero-Rodríguez, S. Nausa, G. de Micheli, R. O'Kennedy, and S. Carrara, "Memristive biosensors based on full-size antibodies and antibody fragments," *Sens. Actuators B, Chem.*, vol. 286, pp. 346–352, May 2019, doi: [10.1016/j.snb.2019.02.001](https://doi.org/10.1016/j.snb.2019.02.001).
- [94] I. Tzouvadaki, N. Aliakbarinodchi, G. De Micheli, and S. Carrara, "The memristive effect as a novelty in drug monitoring," *Nanoscale*, vol. 9, no. 27, pp. 9676–9684, 2017, doi: [10.1039/c7nr01297g](https://doi.org/10.1039/c7nr01297g).
- [95] N. S. M. Hadis, A. A. Manaf, M. F. A. Rahman, S. H. Ngalm, T. H. Tang, M. Citartan, A. Ismail, and S. H. Herman, "Fabrication and characterization of simple structure fluidic-based memristor for immunosensing of NS1 protein application," *Biosensors*, vol. 10, no. 10, p. 143, Oct. 2020, doi: [10.3390/BIOS10100143](https://doi.org/10.3390/BIOS10100143).
- [96] *2017 IEEE Asia Pacific Conference on Postgraduate Research in Microelectronics and Electronics (PrimeAsia)*, IEEE, Piscataway, NJ, USA, 2017.
- [97] H. Duwarah, N. Sharma, J. Devi, K. K. Saikia, and P. Datta, "Memristive approach for estimation of bacterial pathogen *E. coli* concentration using ZnS quantum dots," *Mater. Today, Proc.*, vol. 43, pp. 3891–3895, Jan. 2021, doi: [10.1016/j.matpr.2020.12.1197](https://doi.org/10.1016/j.matpr.2020.12.1197).
- [98] I. Tzouvadaki, F. Puppo, M.-A. Doucey, G. De Micheli, and S. Carrara, "Modeling memristive biosensors," in *Proc. IEEE Sensors*, Busan, South Korea, Nov. 2015, pp. 1–4, doi: [10.1109/ICSENS.2015.7370572](https://doi.org/10.1109/ICSENS.2015.7370572).
- [99] I. Tzouvadaki, F. Puppo, M.-A. Doucey, G. De Micheli, and S. Carrara, "Computational study on the electrical behavior of silicon nanowire memristive biosensors," *IEEE Sensors J.*, vol. 15, no. 11, pp. 6208–6217, Nov. 2015, doi: [10.1109/JSEN.2015.2456336](https://doi.org/10.1109/JSEN.2015.2456336).
- [100] F. Patolsky, G. Zheng, and C. M. Lieber, "Fabrication of silicon nanowire devices for ultrasensitive, label-free, real-time detection of biological and chemical species," *Nature Protocols*, vol. 1, no. 4, pp. 1711–1724, Nov. 2006, doi: [10.1038/nprot.2006.227](https://doi.org/10.1038/nprot.2006.227).
- [101] H. Abunahla, Y. Halawani, A. Alazzam, and B. Mohammad, "NeuroMem: Analog graphene-based resistive memory for artificial neural networks," *Sci. Rep.*, vol. 10, no. 1, p. 9473, Jun. 2020, doi: [10.1038/s41598-020-66413-y](https://doi.org/10.1038/s41598-020-66413-y).
- [102] F. S. Tabar, M. Pourmadadi, F. Yazdian, and H. Rashedi, "Design of electrochemical nanobiosensor in the diagnosis of prostate specific antigen (PSA) using nanostructures," in *Proc. 27th Nat. 5th Int. Iranian Conf. Biomed. Eng. (ICBME)*, Nov. 2020, pp. 35–40, doi: [10.1109/ICBME51989.2020.9319418](https://doi.org/10.1109/ICBME51989.2020.9319418).
- [103] Y.-K. Yen, C.-H. Chao, and Y.-S. Yeh, "A graphene-PEDOT:PSS modified paper-based aptasensor for electrochemical impedance spectroscopy detection of tumor marker," *Sensors*, vol. 20, no. 5, p. 1372, Mar. 2020, doi: [10.3390/s20051372](https://doi.org/10.3390/s20051372).



RAMI HOMSI received the Bachelor of Science degree in mechanical engineering from the University of Sharjah and the Master of Science degree in mechanical engineering from Khalifa University, United Arab Emirates, where he is currently pursuing the Ph.D. degree with the Mechanical Engineering Department. He is also under the close guidance of Dr. Anas Alazzam and Dr. Baker Mohammad. With a passion for using technology to advance the field of healthcare. His current research interest includes the detection of cancer biomarkers using memristors.

NOSAYBA AL-AZZAM received the B.S. degree in dental surgery from the Jordan University of Science & Technology and the M.S. and Ph.D. degrees in biochemistry from The University of Akron, OH, USA. She is currently a highly accomplished and respected biochemist with a wealth of academic and research experience. She is also an Associate Professor in biochemistry with the Jordan University of Science & Technology. Her research interests include exploring the connection between uric acid levels and the development of diabetes and searching for new SNPs related to the uric acid metabolism in diabetic patients and cellular behavior on graphene layers, which hold significant potential for biological and biomedical applications. She is also a member of the Jordan Dental Association and the American Society for Biochemistry and Molecular Biology. She has been honored with numerous awards, including the Peter K. Lauf Travel Award from the Ohio Physiological Society.



BAKER MOHAMMAD (Senior Member, IEEE) received the B.S. degree in ECE from The University of New Mexico, Albuquerque, the M.S. degree in ECE from Arizona State University, Tempe, and the Ph.D. degree in ECE from The University of Texas at Austin, in 2008.

Prior to joining Khalifa University, he was a Senior Staff Engineer/the Manager of Qualcomm, Austin, USA, for six years, where he was engaged in designing high performance and low-power DSP processors used for communication and multi-media application. Before joining Qualcomm, he worked for ten years with Intel Corporation on a wide range of microprocessors design from high performance, server chips > 100Watt (IA-64), to mobile embedded processor low power sub 1 watt (xscale). He has over 16 years of industrial experience in microprocessor design, emphasizing memory, low power circuit, and physical design. He is currently the Director of the System on Chip Center and a Professor in EECS with Khalifa University. He has authored/coauthored over 150 refereed journals and conference proceedings, more than three books, more than 18 U.S. patents, multiple invited seminars/panelists, and the presenter of more than three conference tutorials, including one tutorial on energy harvesting and power management for WSN at the 2015 (ISCAS). His research interests include VLSI, power-efficient computing, high yield embedded memory, and emerging technology, such as memristor, STTRAM, in-memory-computing, and hardware accelerators for cyber-physical systems. He is also engaged in a microwatt range computing platform for wearable electronics and WSN focusing on energy harvesting, power management, and power conversion, including efficient DC/DC and AC/DC converters.

Dr. Mohammad has received several awards, including the KUSTAR Staff Excellence Award in Intellectual Property Creation, the IEEE TRANSACTIONS ON VERY LARGE SCALE INTEGRATION (VLSI) SYSTEMS Best Paper Award, the 2016 IEEE MWSCAS Myrill B. Reed Best Paper Award, the Qualcomm Qatar Award for Excellence on Performance and Leadership, the SRC

Techon Best Session Papers for 2016 and 2017, the 2009 Best Paper Award for Qualcomm Qtech Conference, and Intel Involve in the Community Award for Volunteer and Impact on the Community. He is also an Associate Editor of IEEE ACCESS and IEEE TRANSACTIONS ON VERY LARGE SCALE INTEGRATION (VLSI) SYSTEMS journals. He participates in many technical committees at IEEE conferences and reviews of IEEE TRANSACTIONS ON VERY LARGE SCALE INTEGRATION (VLSI) SYSTEMS and *IEEE Circuits and Systems* magazine.



ANAS ALAZZAM is currently a highly accomplished and recognized scholar in the field of mechanical engineering. As an alumnus with Concordia University, Montreal, Canada, he went on to hold a brief Research Scientist appointment with Canadian Space Agency, before joining Khalifa University, in 2012, where he is currently working as an Associate Professor and the Head of the Microfluidics Laboratory. Furthermore, he holds an affiliate associate professor position with the

Electrical Engineering Department, École de Technologie Supérieure, Montreal, QC, Canada. With expertise in microfluidics, nanofluids, dielectrophoresis, microsystems, phase change materials, and healthcare applications of microdevices. He is the author/coauthor of more than 120 refereed journals and conference proceedings. He has also been an invited Speaker at several distinguished events, including Distinguished Alumni with Concordia University and the IEEE Sensors and Nanotechnology 2019 Conference. He is also a member of the Editorial Board of *Micromachines* and *PLOS One* journals. He has received numerous awards for his outstanding research, including the Faculty Excellence Award from Khalifa University.

...